SF2A 2011
G. Alecian, K. Belkacem, R. Samadi and D. Valls-Gabaud (eds)

RED GIANTS UNVEILED

B. Mosser[1]

Abstract. The CoRoT and Kepler missions provide us with thousands of red giant light curves that allow a very precise asteroseismic study of these objects. Before these space missions, the red giant oscillation patterns remained obscure. Now, these spectra are completely clear. Moreover, they unveil many crucial interior structure properties. For thousands of red giants, we can derive from the seismic data: precise estimates of the stellar mass and radius, the evolutionary status of the giants (with a clear difference between clump and RGB stars), the internal differential rotation, the mass loss, the distance of the stars... Analyzing this large amount of information is made easy by the identification of the largely homologous red giant oscillation pattern. This allows us, for instance, to identify rotation scaling relations, or to measure the mode visibility and the bolometric amplitudes. Fine details completing the red giant oscillation pattern then provide further information for a more detailed view on the interior structure.

Keywords: stars: oscillations, stars: interiors, stars: evolution, stars: late-type, methods: data analysis

1 Introduction

The CNES CoRoT and NASA *Kepler* missions provide us with thousands of high-precision photometric light curves for asteroseismic observations (Michel et al. 2008; Gilliland et al. 2010). A large part of the observed stars are red giants. Their observations have opened a new era in red giant asteroseismology since they give a precise view of pressure modes (p modes), corresponding to oscillations propagating essentially in the large stellar convective envelopes, as well as of mixed modes, corresponding to pressure waves coupled to gravity waves propagating in the core radiative regions.

First ground-based red giant seismic observations were restrained by a 'short' observation duration (of about 1 month) and a poor duty cycle (Frandsen et al. 2002). As a consequence, even if solar-like oscillations were undoubtedly detected, open questions remained, concerning the possible existence of non-radial modes and the measurement of the mode lifetimes in red giants. As a consequence, the physical output of this pioneering work remained unfortunately limited, but motivated a large interest. Red giant seismology has therefore been defined as an objective for the CoRoT and *Kepler* missions.

First CoRoT results on red giants have reported the presence of radial and non-radial oscillations in more than 300 giant stars (De Ridder et al. 2009). They have confirmed the solar-like oscillations, measured mode lifetimes of the order of a month, and found giants with a complex spectrum. This paper aims to summarize the major outputs of these space observations obtained with CoRoT and *Kepler*.

2 Scaling relations

Before addressing the full properties of a red giant oscillation spectrum (Fig. 1), we may focus on the global frequency parameters that describe solar-like oscillations. The central frequency $\nu_{\max}$ of the oscillation power excess is directly related to the photospheric acoustic cutoff frequency; the large separation $\Delta\nu$ of the pressure modes, measuring the travel time of a sound wave along the stellar diameter, is directly related to the mean value of the stellar density. Due to the amount of data, many automated codes have been developed for measuring these parameters (e.g. Mosser & Appourchaux 2009). The different methods have been extensively tested and

[1] LESIA - Observatoire de Paris, CNRS, Université Pierre et Marie Curie, Université Denis Diderot, 92195 Meudon cedex, France; e-mail: benoit.mosser@obspm.fr

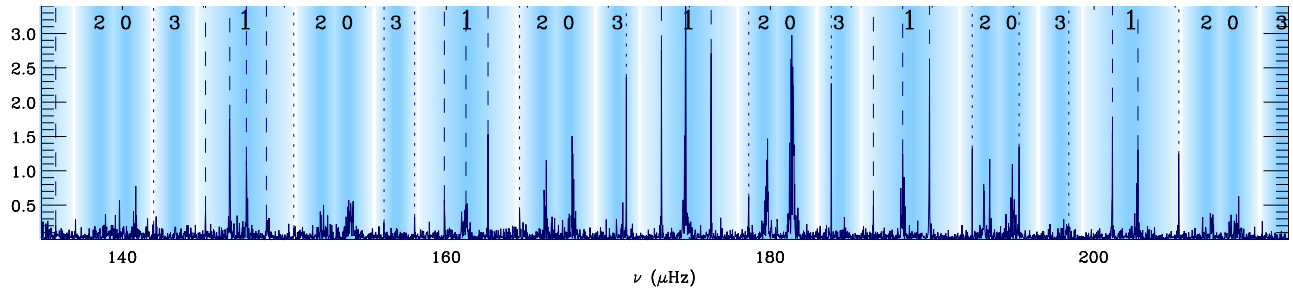

Fig. 1. Power density spectrum of an RGB star observed with *Kepler*. The degrees of the pressure modes are emphasized by the color code. The $\ell = 1$ mixed modes are identified by dashed and dotted vertical lines.

compared (Hekker et al. 2011b; Verner et al. 2011a). Hekker et al. (2009) have shown that $\Delta\nu$ and $\nu_{\rm max}$ are closely related, with a scaling relation of the form

$$\Delta\nu \propto \nu_{\rm max}^{\alpha} \tag{2.1}$$

The value of α is discussed below. The importance of the measurements of $\Delta\nu$ and $\nu_{\rm max}$ is emphasized by their ability to provide accurate estimates of the stellar mass and radius, as theoretically assessed by Belkacem et al. (2011):

$$\frac{R}{R_\odot} = r \left(\frac{\nu_{\rm max}}{\nu_{\rm max,\odot}}\right) \left(\frac{\Delta\nu}{\Delta\nu_\odot}\right)^{-2} \left(\frac{T_{\rm eff}}{T_\odot}\right)^{1/2} \qquad \frac{M}{M_\odot} = m \left(\frac{\nu_{\rm max}}{\nu_{\rm max,\odot}}\right)^{3} \left(\frac{\Delta\nu}{\Delta\nu_\odot}\right)^{-4} \left(\frac{T_{\rm eff}}{T_\odot}\right)^{3/2}. \tag{2.2}$$

The solar values are $\Delta\nu_\odot = 135.5\,\mu$Hz and $\nu_{\rm max,\odot} = 3050\,\mu$Hz, whereas red giant values are much smaller, typically of about 4 and 40 μHz, respectively, at the red clump. Calibration with modelled stars has shown that the factors r and m are very close to 1. On the other hand, observations on cluster stars have proven that r and m have a weak dependence, limited to a few percents, in the evolutionary status (Miglio et al. 2011). Grid modelling reaches similar conclusion (White et al. 2011). As a consequence, mass and radius can be reliably estimated with asteroseismic measurements, with conservative uncertainties of about 15 and 7 % respectively (Fig. 2a). Ongoing modelling will help to significantly reduce the systematic errors, hence the total uncertainties. We stress that these estimates do not depend on any distance measurements.

The scaling relation $M(\nu_{\rm max}, \Delta\nu, T_{\rm eff})$ shows that the exponent of the scaling relation between $\nu_{\rm max}$ and $\Delta\nu$ in Eq. 2.1 is necessarily close to 3/4, since it implies a relation between $\Delta\nu$ and $\nu_{\rm max}$ of the form:

$$\Delta\nu \propto \nu_{\rm max}^{3/4}\ M^{-1/4}\ T_{\rm eff}^{3/8} \tag{2.3}$$

For red giants, Mosser et al. (2010) reported a clear correlation between $T_{\rm eff}$ and $\nu_{\rm max}$: $T_{\rm eff} \propto \nu_{\rm max}^{0.04}$. On the other hand, there is no relation between $\nu_{\rm max}$ and M since all stars ascend the RGB, with a negligible mass loss before the tip, so that one derives for red giant stars $\Delta\nu \propto \nu_{\rm max}^{0.745}$. Observations give very similar results, with an exponent α between 0.745 and 0.764, depending on the method (Huber et al. 2010).

For main-sequence stars, the relation between $\nu_{\rm max}$ and $T_{\rm eff}$ is more steep, and one must take into account the mass dependence in $\nu_{\rm max}$. From previous CoRoT observations (Barban et al. 2009; García et al. 2009; Benomar et al. 2009; Gaulme et al. 2010; Ballot et al. 2011), we estimate that $T_{\rm eff} \propto \nu_{\rm max}^{-0.25}$ and $M \propto \nu_{\rm max}^{-0.70}$, so that $\Delta\nu \propto \nu_{\rm max}^{0.83}$ on the main sequence. This is confirmed by the ensemble-asteroseismic results obtained with *Kepler* (Verner et al. 2011b).

Many other scaling relations between frequency and energy global parameters of the oscillations have been identified (Mosser et al. 2011c, and references therein). These scaling relations are not yet fully understood (e.g. Samadi et al. 2007; Stello et al. 2011). They certainly result from the largely homologous properties of the red giant envelope and also reflect the energy partition between convection and oscillations. The link between granulation and oscillations, both related to the convective flux, has been clearly exposed by Mathur et al. (2011), from *Kepler* observations and 3-D convection simulations. Similarly, Mosser et al. (2011c) have shown that the total energy in the oscillations is proportional to the total energy in the granulation. This emphasizes the interest of the scaling relations for the global understanding of the red giant interior structure.

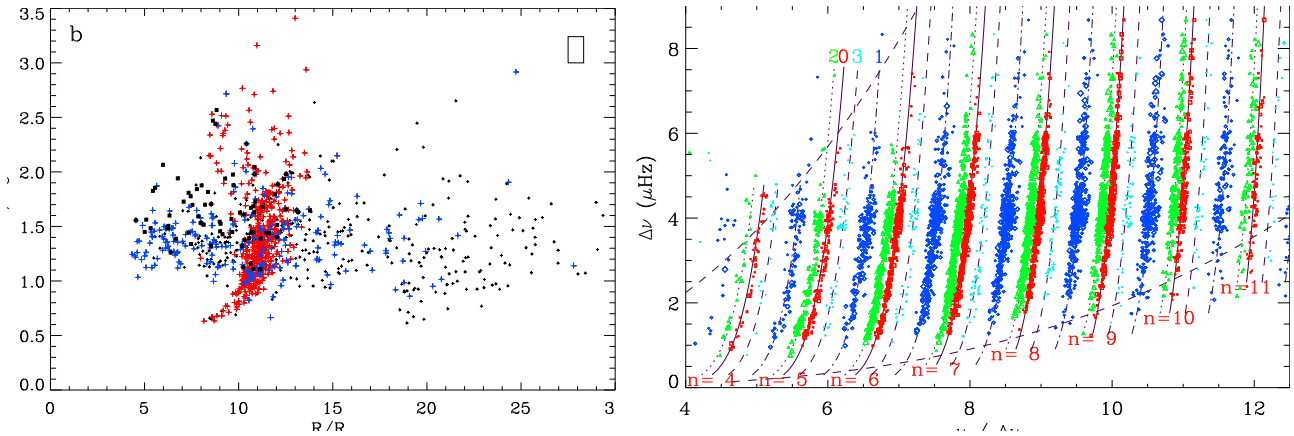

Fig. 2. a: Asteroseismic mass as a function of the asteroseismic radius, from Mosser et al. (2011c). The color code gives the evolutionary status; clump stars in red, giant-branch stars in blue, unknown status in dark grey. The population of giants with very low $\ell = 1$ amplitude is indicated with black squares. The rectangles indicate the mean value of the 1-σ error bars. **b:** Complete identification of the ridges, in red giant oscillation spectra observed with CoRoT and analyzed according to Mosser et al. (2011b). Each colour corresponds to a different mode degree (radial modes in red, dipole modes in dark blue, $\ell = 2$ modes in green, $\ell = 3$ modes in light blue). The dark dashed lines, derived from the scaling law dealing with the oscillation power excess, delineate the region where the modes have noticeable amplitudes (Mosser et al. 2010).

3 The pressure mode oscillation pattern

In this Section, we focus on the p-mode oscillation pattern. Many papers use the simplified form:

$$\nu_{n,\ell} = \left[n + \frac{\ell}{2} + \varepsilon \right] \Delta\nu - d_{0\ell}. \tag{3.1}$$

This form, adapted for red giants from the Tassoul asymptotic relation (Tassoul 1980), introduces mean values of the large separation $\Delta\nu$, of the dimensionless parameter ε, and of the difference $d_{0\ell}$ between non-radial and radial ridges. Various work has shown than all parameters are related to the large separation (Bedding et al. 2010; Mosser et al. 2010; Huber et al. 2010). A refined analysis has shown that a parametrization of the spectrum provides then a very precise measurement of the mean value of the large separation $\Delta\nu$, since it severely reduces the perturbation of the spectrum due to the stochastic excitation of the modes. It also allows an efficient automated identification of the eigenmodes (Fig. 1 and Fig. 2b). The universal red giant oscillation pattern is given by

$$\nu_{n,\ell} = \left[n + \frac{\ell}{2} + \varepsilon(\Delta\nu) - d_{0\ell}(\Delta\nu) + \frac{\alpha}{2} (n - n_{\max})^2 \right] \Delta\nu, \tag{3.2}$$

with $n_{\max} = \nu_{\max}/\Delta\nu$. The constant α, close to 0.008 for radial modes (Mosser et al. 2011b), accounts for the fact that the spacing between consecutive radial eigenfrequencies linearly varies with frequency. As a consequence, the mean large separations introduced by Eqs. 3.1 and 3.2 are not strictly equivalent. In practice, they are very close from each other, and different but very close (about 1 %) to the definition related to the stellar acoustic diameter ($\Delta\nu = (2\int_0^r \mathrm{d}r/c)^{-1}$, with c the sound speed) which is considered in the mass and radius scaling relations.

With high-resolution oscillation spectra, it is now possible to investigate a more precise description of the local values of the large separations $\Delta\nu(\nu)$, defined as the spacing between consecutive eigenfrequencies with the same degree ℓ. A systematic modulation in the spectrum was early put in evidence (Mosser et al. 2010). The measurement of $\Delta\nu(\nu)$ for radial modes only (Mosser 2010) allows us to measure the modulation of the large separation due to the helium second-ionization region (Miglio et al. 2010).

4 Mixed modes

Mixed modes correspond to waves propagating as pressure waves in the convective envelope, and as gravity waves in the radiative region of the core. Such modes, with a huge number of nodes inside the core, are able

to analyze in great detail its structure. Their theoretical description can be found in Dupret et al. (2009) and references therein.

In red giants, they were first reported by Beck et al. (2011). The analysis by Bedding et al. (2011) and Mosser et al. (2011a) has shown that they are sensitive to the stellar evolutionary status, and allow us to make a clear difference between RGB stars (with an inactive helium core) and clump stars (burning the central helium). Recent work by Mosser et al. (2011c) shows that the mixed modes also precisely probe the thin shell where hydrogen is burning. Very different mixed-modes spectra are observed, which probably correspond to various situations occurring during the red giant evolution. Mosser et al. (2012) have shown that the mixed-mode eigenfrequency pattern can be modelled with a formalism close to what has been developed for pure p or g modes (Tassoul 1980). This is of great interest for identifying the mixed modes, since the coupling severely complicate their pattern. With the identification of mixed modes in a wide frequency range, we can now propose a direct measure of the g-mode spacing. This gives, for the first time, a clear insight on the red giant core. The mixed modes also directly probe the region where hydrogen burns in shell.

5 Mass loss, populations, red giants in cluster

With space-borne observations, asteroseismic observations now directly constrain the interior structure. We can for instance read in the radius-mass diagram shown in Fig. 2 the signature of the mass loss occurring at the tip of the red giant branch. Most of the stars ascending the RGB have a mass in the range $[1, 2\,M_\odot]$. Lower mass stars are more rare, since they take time to evolve on the main sequence; higher mass stars evolving rapidly are rare too. After the tip (not yet probed by the data, due to a limit in frequency resolution), the distribution of the stellar mass in the clump starts at $0.6\,M_\odot$. This means that significant mass loss has occurred at the tip of the RGB. We also note that the mass-radius relation is well defined for clump stars in the range $[0.6, 1.8\,M_\odot]$. The RGB progenitors of these stars had a degenerate helium core, so that the helium ignition started abruptly. As a consequence of the helium flash, the cores of these stars have very similar masses and physical conditions; the equilibrium state of the envelope then yields the mass-radius relation. Above $1.8\,M_\odot$, stars of the secondary clump have avoided the helium flash. Hence, the spread in the mass-radius relation is more important than for red-clump stars.

As a direct consequence of the measurement of the stellar radius (Eq. 2.2), the luminosity of the star can be derived from the Boltzmann law, hence its absolute magnitude and its distance. This allows us to probe the stellar population, especially in the different fields of CoRoT, with small galactic latitudes (Miglio et al. 2009). Red giants are also observed in clusters (Basu et al. 2011; Hekker et al. 2011a), with specific consequences due to the advantage of observing stars with similar age and initial composition (Stello et al. 2011).

6 A golden age for red giant asteroseismology

Many topics have not been developed in this rapid review on asteroseismology. A more complete view was given by Bedding (2011). It is worth noting that the modelling of individual stars has just started (Jiang et al. 2011; di Mauro et al. 2011). At the moment, grid modelling is prevailing (e.g. Kallinger et al. 2010). This means that the physics of the models is not specifically addressed. This will be done in a near future, for making the best of asteroseismic constraints, as already shown by Miglio et al. (2010) who showed how the modulation of the large separation directly probes the helium second-ionization region. A direct investigation of the physical conditions in the helium core will be provided by the mixed modes (Mosser et al. 2011c). Furthermore, the way these mixed modes are coupled to the pressure modes will test the shell where hydrogen is burning.

In the future, CoRoT observations are necessary to provide population studies, as shown by Miglio et al. (2009), with access to young populations in the Galactic disk not observed by *Kepler*. On the other hand, *Kepler* observation will benefit from a 4-year long duration, providing very high SNR spectra. They will give access to the inner rotation profile (Beck et al., accepted in Nature) and to the tip of the RGB, with a possible connection with ground-based observations (Dziembowski & Soszyński 2010).

The CoRoT space mission, launched 2006 December 27, was developed and is operated by the CNES, with participation of the Science Programs of ESA, ESAs RSSD, Austria, Belgium, Brazil, Germany, and Spain. Funding for the Discovery *Kepler* mission is provided by NASA's Science Mission Directorate. We gratefully acknowledge the entire CoRoT and *Kepler* teams, whose efforts have made these results possible.

References

Ballot, J., Gizon, L., Samadi, R., et al. 2011, A&A, 530, A97
Barban, C., Deheuvels, S., Baudin, F., et al. 2009, A&A, 506, 51
Basu, S., Grundahl, F., Stello, D., et al. 2011, ApJ, 729, L10
Beck, P. G., Bedding, T. R., Mosser, B., et al. 2011, Science, 332, 205
Bedding, T. R. 2011, ArXiv e-prints
Bedding, T. R., Huber, D., Stello, D., et al. 2010, ApJ, 713, L176
Bedding, T. R., Mosser, B., Huber, D., et al. 2011, Nature, 471, 608
Belkacem, K., Goupil, M. J., Dupret, M. A., et al. 2011, A&A, 530, A142
Benomar, O., Baudin, F., Campante, T. L., et al. 2009, A&A, 507, L13
De Ridder, J., Barban, C., Baudin, F., et al. 2009, Nature, 459, 398
di Mauro, M. P., Cardini, D., Catanzaro, G., et al. 2011, MNRAS, 415, 3783
Dupret, M., Belkacem, K., Samadi, R., et al. 2009, A&A, 506, 57
Dziembowski, W. A. & Soszyński, I. 2010, A&A, 524, A88
Frandsen, S., Carrier, F., Aerts, C., et al. 2002, A&A, 394, L5
García, R. A., Régulo, C., Samadi, R., et al. 2009, A&A, 506, 41
Gaulme, P., Deheuvels, S., Weiss, W. W., et al. 2010, A&A, 524, A47
Gilliland, R. L., Brown, T. M., Christensen-Dalsgaard, J., et al. 2010, PASP, 122, 131
Hekker, S., Basu, S., Stello, D., et al. 2011a, A&A, 530, A100
Hekker, S., Elsworth, Y., De Ridder, J., et al. 2011b, A&A, 525, A131
Hekker, S., Kallinger, T., Baudin, F., et al. 2009, A&A, 506, 465
Huber, D., Bedding, T. R., Stello, D., et al. 2010, ApJ, 723, 1607
Jiang, C., Jiang, B., Christensen-Dalsgaard, J., et al. 2011, ArXiv e-prints
Kallinger, T., Mosser, B., Hekker, S., et al. 2010, A&A, 522, A1
Mathur, S., Hekker, S., Trampedach, R., et al. 2011, A&A, in press
Michel, E., Baglin, A., Auvergne, M., et al. 2008, Science, 322, 558
Miglio, A., Brogaard, K., Stello, D., et al. 2011, ArXiv e-prints
Miglio, A., Montalbán, J., Baudin, F., et al. 2009, A&A, 503, L21
Miglio, A., Montalbán, J., Carrier, F., et al. 2010, A&A, 520, L6
Mosser, B. 2010, Astronomische Nachrichten, 331, 944
Mosser, B. & Appourchaux, T. 2009, A&A, 508, 877
Mosser, B., Barban, C., Montalbán, J., et al. 2011a, A&A, 532, A86
Mosser, B., Belkacem, K., Goupil, M., et al. 2010, A&A, 517, A22
Mosser, B., Belkacem, K., Goupil, M. J., et al. 2011b, A&A, 525, L9
Mosser, B., Elsworth, Y., Hekker, S., et al. 2011c, ArXiv e-prints
Mosser, B., Goupil, M., Belkacem, K., et al. 2012, submitted to A&A
Samadi, R., Georgobiani, D., Trampedach, R., et al. 2007, A&A, 463, 297
Stello, D., Huber, D., Kallinger, T., et al. 2011, ApJ, 737, L10
Tassoul, M. 1980, ApJS, 43, 469
Verner, G. A., Elsworth, Y., Chaplin, W. J., et al. 2011a, MNRAS, 415, 3539
Verner, G. A., Elsworth, Y., Chaplin, W. J., et al. 2011b, MNRAS, 892
White, T. R., Bedding, T. R., Stello, D., et al. 2011, ArXiv e-prints